ISSN (Print) 1226-1750
ISSN (Online) 2233-6656
Journal of Magnetics 27(1), 35-41 (2022) https://doi.org/10.4283/JMAG.2022.27.1.035

First Principles Investigation on Electrically Controlled Magnetic Moments of Ultrathin Palladium Film on MgO(001)

Tran Van Quang[1,2], Hanchul Kim[3,4], and Miyoung Kim[3]*

[1]*Faculty of Electronics and Telecommunications, VNU University of Engineering and Technology, Hanoi, Vietnam*
[2]*Department of Physics, University of Transport and Communications, Hanoi, Vietnam*
[3]*Department of Applied Physics, Sookmyung Women's University, Seoul 04310, Republic of Korea*
[4]*Korea Institute for Advanced Study, Seoul 02455, Republic of Korea*

(Received 21 February 2022, Received in final form 22 March 2022, Accepted 23 March 2022)

Electric field dependence of magnetic, electronic, and structural properties in a Pd bilayer film on MgO (001) is investigated by using the first-principles electronic structure calculations within density functional theory. We find that, due to the lattice mismatch of 6.7 %, a ferromagnetic ground state is stabilized at zero electric field on an otherwise paramagnetic Pd with the spin magnetic moments of m = 0.31 and 0.34 μ_B in surface and interface Pd, respectively. The application of an external electric field, E, causes the Pd magnetic moments to be modulated in a site- and electric field-dependent manner. As the external electric field pointing inward to the Pd surface is increased up to the critical value of 1.3 V/Å, the surface Pd moment is barely changed while the interfacial Pd moment increases linearly with E. Above this critical electric field, the moments of both the interfacial and surface Pd atoms exhibit nonlinear increase with E and reach up to 0.34 (surface) and 0.41 (interface) μ_B at E = 2.5 V/Å. When the electric field direction is inverted, a similar dependence on E is obtained for both Pd atoms at the critical electric field value of −0.5 V/Å. The peculiar behavior of the induced magnetic moments is explained by combining the linearized Stoner and itinerant conduction models. We reveal that this prominent magnetoelectric effect is due to the modulated charge occupancy of Pd 4*d*-states in the minority spin channel in which the d_{z^2} and $d_{x^2-y^2}$ orbitals play crucial roles.

Keywords : palladium, thin film, magnetism, electronic structure, first-principles calculation, magnetoelectric effect, magnetic moments, density of states

1. Introduction

Controlling magnetism with non-magnetic means via the magnetoelectric (ME) effect has drawn substantial attention for decades owing to its potential applications in magnetic data storage and spintronics device technology [1-3]. While early research has focused on materials such as multiferroics or magnetic semiconductors with *intrinsic* ME coupling, more recent studies have focused on tailoring the magnetic properties of various materials locally by using *extrinsic* methods such as external electric fields or doped charges. The ME effect governs the induction as well as modification of magnetization by electric fields and results in many exotic phenomena such as electrically controlled surface/interfacial magnetization, magnetic ordering, exchange bias, magnetocrystalline anisotropy (MCA), and the effect of ferroelectricity on spin transport [4-9]. Among the various mechanisms that drive ME coupling under electric fields, the two most frequently studied ones that have purely electrical origins are the strain effect and interatomic bonding modulation. In the former, the charge redistribution due to the displacement of ions from their original positions plays a crucial role and is known to modify the magnetization in multiferroics via the magnetostrictive response. In the latter, focus is placed on the modulated bonding between atoms across an interface due to polarization changes (or even inversion), especially in ferroelectric interfaces [10-12].

One of the most investigated systems in this field are transition metal surfaces/interfaces which exhibit unique magnetic properties even without an external electric field, such as the enhancement of the magnetization and MCA, as well as peculiar magnetic phase transitions that

*Corresponding author: Tel: +82-2-2077-7077
Fax: +82-0303-0799-0362, e-mail: mykim.nu@gmail.com

depend sensitively on the atomic environment [13]. When a transition metal is exposed to an external electric field, spin-dependent conduction charge screening gives rise to a substantial ME effect. The electrons in the metal surface/interface redistribute efficiently to screen out the electrostatic force due to the external field. This charge redistribution differs between the spin-up and spin-down channels, and therefore alters the spin densities and magnetic properties. Early research has reported a *linear dependence* of the magnetic moments on the external electric field at the Fe and Co surfaces/interfaces in free-standing monatomic films [10] as well as in overlayers on various substrates such as Fe/MgO [14], MgO/Fe/X (X = Pt, Au) [15], FeCo/MgO [16], and Fe/$BaTiO_3$ [17]. This *linear* behavior has been explained mainly through a simple rigid band model with a spin-dependent Fermi energy perturbation and a field-induced modification of the *d*-orbitals [10, 18, 19]. More interestingly, a *nonlinear dependence* of the induced magnetic moments on the external electric field was reported in free-standing monatomic Pd thin films and in Pd overlayers on Ag or BaO substrates. The nonlinear dependence was explained by the rigid-band model in combination with a linearized Stoner model [20-22].

The Stoner model, together with first-principles band calculations, provides a feasible theoretical framework to explain how itinerant ferromagnetism is stabilized in metals through the density of states (DOS) at the Fermi energy. Palladium is one of the most interesting metals to be investigated using this framework. Pd has a paramagnetic (PM) ground state in the bulk phase and exhibits a variety of interesting magnetic characteristics because it has the highest magnetic susceptibility among single-element metals and a large DOS peak at the Fermi energy at the verge of Stoner's criterion [23]. For example, a lattice expansion of 4-6 % induces a ferromagnetic (FM) ground state in the Pd bulk and magnetization in lattice-mismatched Pd thin films deposited on substrates in which the DOS peak of the highly localized Pd *d*-orbital at the Fermi energy and the quantum confinement effect play crucial roles [24-26] .

In this work, we carry out first-principles calculations on a Pd bilayer film on a MgO (001) substrate to explore the ME effect on the magnetic moments. MgO is an appropriate substrate for enhanced ME coupling in a Pd film owing to its relatively large lattice constant and high permittivity. By introducing an external electric field perpendicular to the film and investigating its effects on the electronic, structural, and magnetic structures, we demonstrate that the FM ground state is induced in the Pd bilayer on MgO even without an external electric field and the induced Pd surface/interface magnetic moments are significantly modulated by external electric fields exhibiting mixture of linear and nonlinear characteristics as well as a clear site dependence. This prominent ME effect is ascribed to the enhanced screening charge due to a large dielectric constant at interface as well as the spin dependent modulation of the charge occupancy of the Pd 4*d*-states, among which the d_{z^2} and $d_{x^2-y^2}$ orbitals in the minority spin channel are playing especially important roles.

2. Structures and Methods

We performed first-principles electronic structure calculations within the density functional theory (DFT) using the projector augmented wave potentials implemented in the Vienna *ab-initio* simulation package [27-29]. The local density approximation (LDA) was employed for the exchange-correlation functional because the drastically overestimated equilibrium lattice constant under the generalized gradient approximation leads to the prediction of a spurious FM ground state in bulk Pd [30, 31]. A kinetic energy cut-off of 450 eV for the plane-wave basis set and a 40 × 40 × 1 Monkhorst-Pack k-point grid for the three-dimensional first Brillouin zone integration were used.

Figure 1 shows the side view of the Pd/MgO (001) slab used in this study. The unit cell consists of two atomic Pd layers epitaxially deposited on a MgO(001) substrate with three atomic layers. The interfacial (I) Pd atom is located on top of the oxygen in the interfacial MgO layer, which has been reported to be the preferred site for Pd adatoms in previous experimental and theoretical studies [32]. We fixed the (001) in-plane lattice constant to that of the

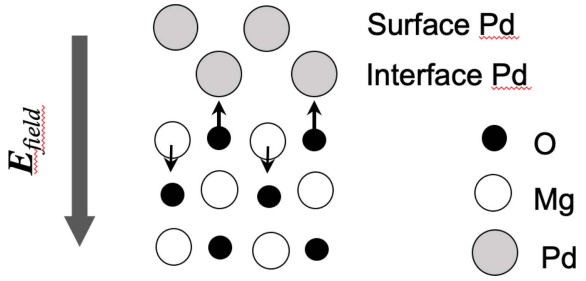

Fig. 1. Side view of Pd/MgO (001) slab used in this work. The external electric field, E_{field}, is applied perpendicular to the film. For convenience, we regard the applied electric field as positive when it points inward (from the Pd surface to the substrate), as depicted by the thick arrow. The small arrows on the atoms indicate the direction of the most significant atomic displacements due to the positive electric field obtained by structural optimization.

MgO substrate obtained by using LDA, that is, a_{MgO} = 4.15 Å. This implies an in-plane lattice expansion of the Pd layers by about 6.7 % from the bulk lattice constant, a_{Pd} = 3.89 Å [30,33]. A 16 Å thick vacuum region was inserted between the repeated slabs along the [001] out-of-plane direction to avoid interaction between the slabs. Under this constraint, the vertical atomic positions were fully relaxed until the Hellmann-Feynman atomic forces along the [001] direction were less than 5.0 meV/Å. An external electric field (E) was introduced along the perpendicular direction of the slab using the dipolar layer method [34]. For convenience, the electric field direction is considered as *positive* when it is oriented *inward*, that is, from the Pd surface to the substrate, as shown in Fig. 1. We further relaxed the vertical atomic positions before and after imposing the electric field to obtain a fully optimized structure. The arrows on the interfacial O and Mg atoms in the figure indicate the directions of the atomic displacement due to a *positive* electric field. The electric field-induced atomic displacements of the other atoms were found to be negligible (less than 10^{-2} Å) for electric field strengths of up to 2.5 V/Å.

3. Results and Discussion

In Fig. 2, we plot the projected density of states (PDOS) of the Pd 4*d* states at the (a) surface and (b) interfacial layers for the spin-up and spin-down channels for E = 0.0 (dotted lines), 2.0 (red solid lines), and –2.0 (blue solid lines) V/Å. While the PDOS profiles of the spin-up and spin-down channels look similar, we observe a clear exchange splitting and large DOS peaks near the Fermi energy E_F, which imply that a stable ferromagnetism exists even before the external electric field is applied. Indeed, our calculations reveal that the ground state of Pd/MgO (001) is ferromagnetic at zero field (E = 0.0 V/Å) with Pd spin magnetic moments of 0.31 and 0.34 μ_B at the surface (S) and interface (I), respectively. The magnetic moments of the other atoms are negligible except for the 0.02 μ_B of the interfacial oxygen which is due to the proximity-induced magnetism of the O 2*p* states. The induced ferromagnetism of the Pd bilayer stems partly from the in-plane lattice expansion due to the lattice mismatch of 6.7 % and partly from the band narrowing due to the surface/interface effect [24]. This result agrees with previous reports on the magnetic moments of Pd surfaces [35-39]. We find that the spin-down channels have a PDOS spike located right at E_F, which implies that the minority-spin electrons are dominant near the Fermi level and may play a major role in field-induced charge redistribution.

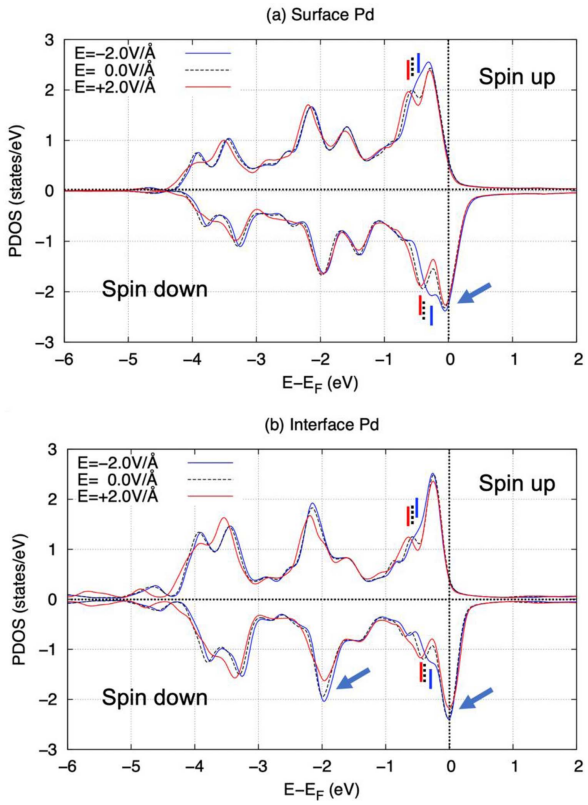

Fig. 2. (Color online) Calculated projected density of states (PDOS) of the (a) surface and (b) interfacial Pd d-states of Pd/MgO (001) for the spin up and spin down channels. The dotted lines are the results with zero external electric field. The blue and red lines are results with an external electric field of –2.0 and 2.0 V/Å, respectively E_F stands for the Fermi energy. Short vertical lines are added to denote the gradual peak position change due to the electric fields.

Upon the application of an external electric field of E = 2.0 V/Å, we observe two main field-induced changes in the PDOS that appear more clearly in the interfacial Pd than in the surface Pd. The first change occurs in the low-energy region of $-6 \lesssim E - E_F \lesssim -3$ (eV) because of enhanced hybridization with the O 2*p* states. This is closely related to the field-induced structural optimization. As shown in Fig. 1, we find that the interfacial O under Pd (I) is pushed up by the inward electric field, as expected from the negative charge of the ion. As a result, the interatomic distance between interfacial O and Pd (I) decreases by about 1 % at E = 2.0 V/Å, which results in an enhanced hybridization between the Pd (I) 4*d* and O 2*p* states. However, this modulation is spin independent; therefore, its influence on the magnetic moment is negligible. The second PDOS change by the electric field occurs near E_F and is due to the screening of the electric field by conduction electrons. We observe that the peak

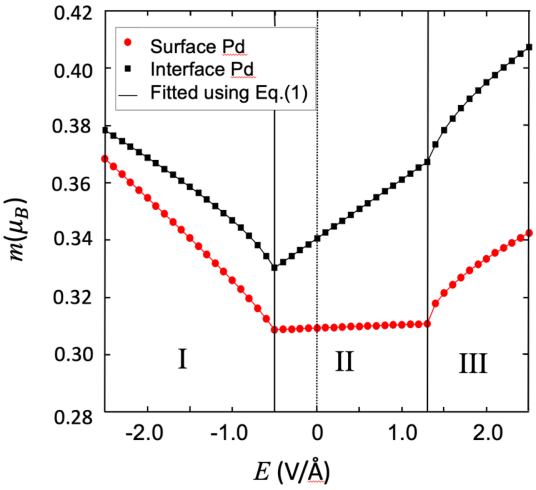

Fig. 3. (Color online) Calculated spin magnetic moments, m, (in μ_B) of Pd atoms at the surface (S) (circles) and interfacial (I) (squares) layers of Pd/MgO (001) as functions of the electric field, E (in V/Å). The solid lines represent the magnetic moments fitted using Eq. (1). Pronounced offsets are found at the two critical electric field values of $E_{c1} = -0.5$ and $E_{c2} = 1.3$ V/Å.

values of the PDOS are reduced slightly for both spin channels and, at the same time, the position of the DOS peaks and the band widths are also changed from those of the zero-field case. These electric field-induced band modulations occur more clearly in interfacial Pd than in surface Pd, as can be seen by comparing the PDOS indicated by arrows. As expected, our calculation reveals that the Pd magnetic moments induced by the $E = 2.0$ V/Å electric field increase by 0.02 μ_B and 0.06 μ_B at the surface and interface, respectively. We show PDOS for negative electric field of $E = -2.0$ V/Å for comparison.

We now vary the external electric field from –2.5 to 2.5 V/Å. Figure 3 shows the calculated spin magnetic moments of Pd at the surface (S) layer as circles and those at the interface (I) layer as squares as functions of the electric field field E. As mentioned above, the Pd magnetic moments increase from 0.31 (S) and 0.34 (I) μ_B at $E = 0$ – 2.0 V/Å to 0.33 and 0.40 μ_B at $E = 2.0$ V/Å, respectively. We find that both the surface and interface magnetizations are substantially modulated by external electric fields but show different characteristics depending on the strength and direction of the electric field. In particular, both layers exhibit significant offsets of their magnetic moments at the two critical electric field values of $E_{c1} = -0.5$ V/Å and $E_{c2} = 1.3$ V/Å.

We first discuss the magnetic moments of the surface layer. The application of electric fields with $E_{c1} \leq E \leq E_{c2}$ (region II in Fig. 3) does not change the magnetic moments at the surface (S), which remain at the same value as that at zero field, i.e., 0.31 μ_B. When the strength of the applied field is increased in the positive direction above E_{c2} (region III) or in the negative direction below E_{c1} (region I), the magnetic moments increase nonlinearly with the electric field. In comparison, the Pd surface in a Pd/Ag (001) film maintains a PM state up to the critical electric field of 1.5 V/Å and then undergoes a transition to a FM state above the critical field with a nonlinear increase of the magnetic moments with E [20]. For interfacial Pd, on the other hand, Figure 3 demonstrate that the magnetic moments change linearly with electric fields of $E_{c1} \leq E \leq E_{c2}$ in region II. From the linear fit of the induced magnetic moments to the electric field, we obtain a slope of 0.02 μ_B per V/Å. A linear dependence of magnetization on the electric field with the same order of slope have also been found in a freestanding Fe film [10]. While the linear increase of surface magnetization is restricted on a surface layer for metal Fe film, our results show that the interface Pd moments also show a strong linear dependence on the electric field. This indicates that the induced interface charge density $\varepsilon = \varepsilon_0 \varepsilon E$ which linearly scales with dielectric constant ε is enhanced at Pd/MgO interface due to the large dielectric constant of MgO and unequally distributed between the spin up and down states. When the strength of the electric field increases beyond the critical values in each direction (regions I and III), a pronounced transition from a linear to a nonlinear dependence of the magnetic moments on the electric field is observed.

To describe both the linear and nonlinear dependence, we assume that the induced magnetic moment, $\Delta m(E) = m(E) - m(E = 0)$, can be described as a combination of a linear term [10] and a square-root term [20], i.e.,

$$\Delta m(E) = a_i^{(S,I)}(E - E_{cj}) + b_i^{(S,I)}\sqrt{E - E_{cj}}, \qquad (1)$$

where i represents the region of E (I, II, or III in Fig. 3), and E_{cj} is the critical value of either E_{c1} or E_{c2}. The coefficients a_i describe the linear behavior of m that originates from the spin-dependent shift of the DOS around the Fermi energy, as found in 2D ferromagnetic materials such as Fe, CrO_2, and Fe/MgO [13]. The nonlinear term arises from the spin-dependent shift of DOS around the Fermi energy while obeying the charge conservation which gives rise to the square-root dependence of the total exchange-driven shifts, i.e. an exchange splitting, of majority and minority spins as a function of DOS at Fermi energy. Moreover, DOS at Fermi energy is perturbed due to the electric field and the fluctuation the can be written as a linear function E field whereas the stabilized ferromagnetism is achieved if the magnetic moment is proportional to the exchange splitting [20].

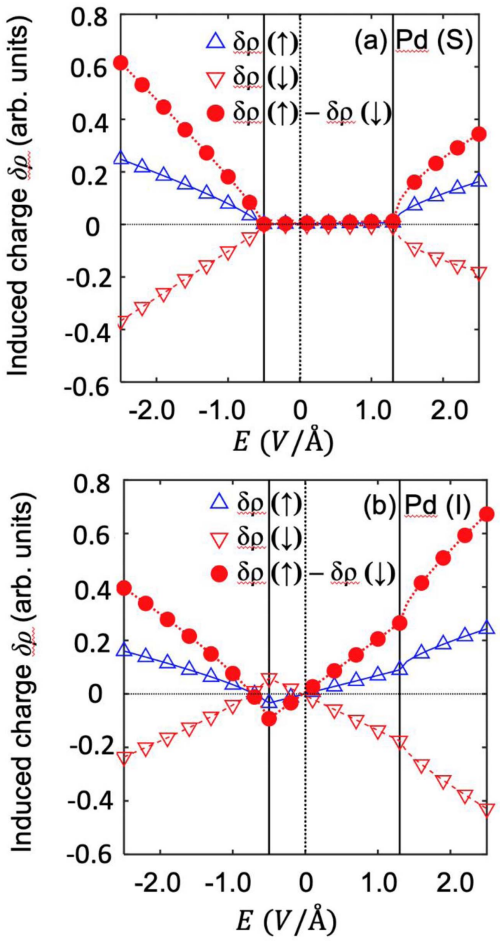

Fig. 4. (Color online) The induced charge of the *d*-states, $\delta\rho = \rho(E) - \rho(0)$(in arbitrary units) for the (a) surface Pd (S) and (b) interfacial Pd (I) layers are shown for the majority (in up-triangles) and minority spins (in down-triangles). The induced spin density given by their difference, $\delta\rho(\uparrow) - \delta\rho(\downarrow)$, is also shown (in circles).

Together with the Stoner criterion, the overall effect leads to the square-root behavior which is represented by the coefficient b_i in Eq. (1). For region III, where the predominant effect is mainly from the nonlinear term, as is also the case in Pd/Ag(001) thin film, the estimated coefficients are $b_{III}^{(S)} = 0.023$ for the surface and $b_{III}^{(I)} = 0.033$ for the interface (in μ_B Å$^{1/2}$V$^{-1/2}$). In region I, we obtain the fitted parameters of $a_I^{(S)} = 0.020$, $a_I^{(I)} = 0.011$ (in μ_B Å/V) and $b_I^{(S)} = 0.011$, $b_I^{(I)} = 0.020$ (in μ_BÅ$^{1/2}$V$^{-1/2}$) under the assumption that both the linear and nonlinear terms play roles. The solid lines in Fig. 3 show the fitted results for $m(E)$ using Eq. (1). We find that the equation describes the calculated electric field dependence of the Pd magnetic moments very well.

One origin of the electric field-induced magnetism in ferromagnetic metals is the spin-dependent change in charge occupancy in response to the external field due to exchange splitting. In Figure 4, we show the induced charge of the Pd 4*d*-bands, $\delta\rho$, obtained by comparing the disturbed ($E \neq 0$) and undisturbed ($E = 0$) charges, that is, $\delta\rho = \rho(E) - \rho(E = 0)$ for (a) surface and (b) interfacial Pd. The induced charges for the majority (↑) and minority spin $\delta\rho(\downarrow)$ are denoted by the upward and downward triangles, respectively. The induced spin densities, $\delta\rho(\uparrow) - \delta\rho(\downarrow)$, are also presented as filled circles for comparison. Overall, we find that the induced spin densities come from the combination of a decrease in the majority spin charge and an increase in the minority spin charge with the applied electric field. On the other hand, the total induced charge, $\delta\rho(\uparrow) + \delta\rho(\downarrow)$, (while not shown in the figure) has negative values in surface Pd for negative electric field and in interface Pd for positive electric field when the magnitude of electric field is over the critical value, which indicates that an environment dependent charge depletion occurs due to the external electric field.

By decomposing the induced charges into the five 4*d*-orbitals, we find that the orbitals processing large PDOS peaks at Fermi energy play important roles in megneto-electric effect. The orbital-decomposed induced charges are shown in Fig. 5 for (a) surface and (b) interfacial Pd. Please note that $\delta\rho$ for (a) and (b) are in different scales. The PDOS of five 4*d*-orbitals are also presented on right panels for (c) surface and (d) interfacial Pd. For surface Pd, we can see that the constant magnetic moments in region II are the result of the small induced charges for each spin and orbital, which add up to zero. The prominent field-induced magnetic moments in regions I and III are mainly due to the decrease in the minority spin charges in the d_{z^2} and $d_{x^2-y^2}$ orbitals, respectively. The second-order transition to a nonlinear field dependence at $E_{c2} = 1.3$ V/Å is particularly governed by the spin minority $d_{x^2-y^2}$ and the spin majority d_{xy} orbitals.

In contrast, for the interface layer (Fig. 5(b)), the induced charge density in the d_{z^2} orbital for the minority spin channel plays a crucial role in determining the field-induced magnetic moments. In region II, the induced electronic charge density in the d_{z^2} orbital for the minority spin undergoes a drastic linear decrease as the electric field increases, which results in a linear increase in the induced magnetic moments with the field. The pronounced offsets at the critical electric field values of E_{c1} and E_{c2} and the nonlinear dependence on the electric field in regions I and III are also found to be unique characteristics of the d_{z^2} components in the minority-spin channel. We observe that the spin minority $d_{x^2-y^2}$ for surface and d_{z^2} for interfacial Pd exhibit the dominant PDOS peaks at Fermi energy as indicated by arrows in (c) and (d) and

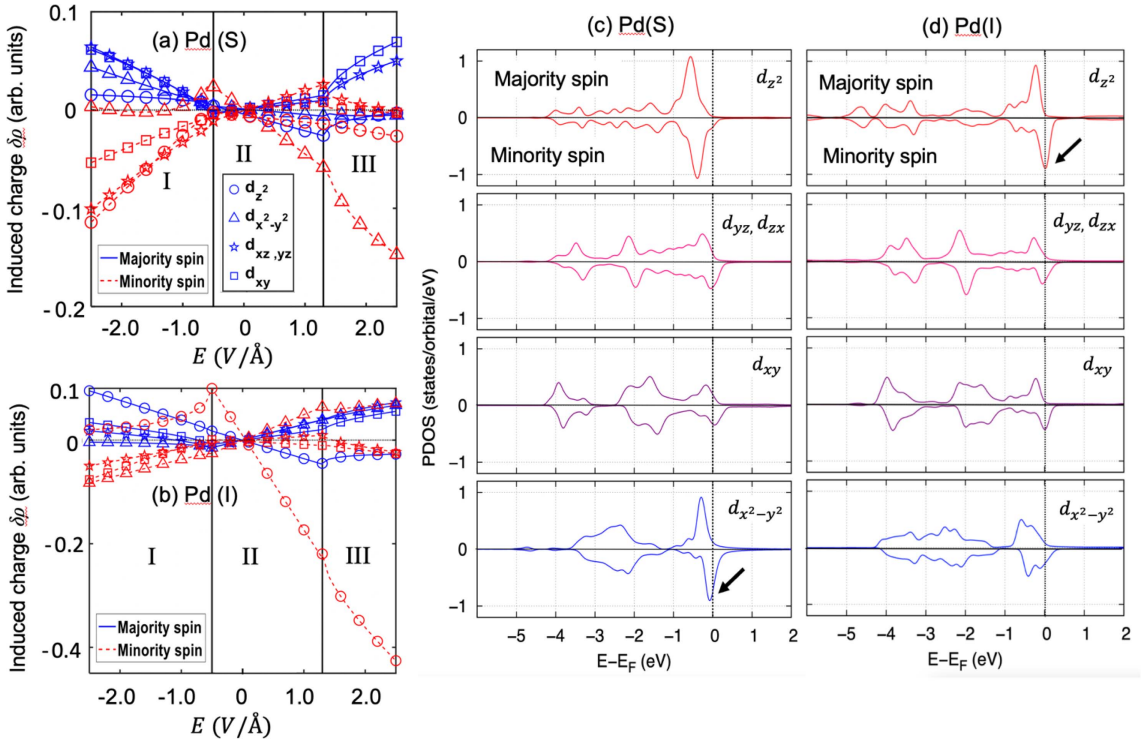

Fig. 5. (Color online) Orbital-decomposed induced charge, $\delta\rho = \rho(E) - \rho(0)$ (in arbitrary units), of the d_{z^2} (circles), $d_{x^2-y^2}$ (triangles), d_{xy} (squares) and $d_{xy,yz}$ (stars) orbitals for the (a) surface and (b) interfacial Pd 4*d* states are shown in left panels. Spin majority results are shown in blue and connected by solid lines while spin minority results are in red and dotted lines. Note that $\delta\rho$ for (a) and (b) are in different scales for easy comparison. Also, the orbital-decomposed DOS are shown in right panels for (c) surface and (d) interfacial Pd 4*d* states.

thus play important roles for magnetoelectric effect of present system, whereas all orbitals contribute to different extents. While our result provides the detailed discussion on which *d*-orbital is mostly responsible for the magnetoelectric effect for present system, it is still to be desired to understand why there is an "onset" of the magnetism that triggers a nonlinear behavior.

We find that the results are hardly dependent on the substrate thickness, which is consistent with other reports [38]. Indeed, we carried out calculations in which the thickness of the MgO layers was increased to up to five atomic layers and obtained qualitatively similar dependences of the magnetization on the electric field with the same critical electric field values of $E_{c1} = -0.5$ and $E_{c2} = 1.3$ V/Å. As mentioned above, we fully relaxed the vertical atomic positions by varying the electric field values to account for the ion relaxation effect, which is known to play a critical role in ME materials, including dielectric interfaces. The most prominent displacements due to the electric field are found in the interfacial Mg^+ and O^- ions, which relax in opposite directions to each other, as shown in Fig. 1. The displacements of the surface and interfacial Pd atoms due to the electric field are relatively negligible. The optimization results in a reduction of the interatomic distance between the interfacial Pd and oxygen, as mentioned earlier. However, we find that effect of these relaxations on the magnetization of the film is not critical, that is, ionic relaxations are not responsible for the electric field-induced magnetic moment in the present film. This was confirmed in our hypothetical calculations with unrelaxed atomic positions (not shown here).

4. Conclusion

We studied the effects of external electric fields on the magnetic moments of a Pd bilayer deposited on MgO (001) substrates using first-principle DFT calculations. Our results show that the external electric field induces a significant site- and field-dependent change in the thin film magnetization. The magnetic moment of interfacial Pd increases linearly with the field while that of surface Pd barely changes when the electric field is between the two critical values of –0.5 and 1.3 V/Å. When the electric field strength increases in the positive direction beyond the upper critical value or in the negative direction below the lower critical value, both the surface and interfacial

magnetic moments undergo a second-order transition from a linear to a nonlinear increase with the electric field. We find that the origin of this peculiar feature is the spin- and orbital-dependent modulation of the induced charges of the Pd *d*-states. Particularly, electric field dependence of the interfacial Pd moments is governed by a significant reduction in the charge occupancy of the minority-spin d_{z^2} orbital. The ME effect in ferromagnetic metal surfaces is mostly localized within the first atomic layer on the surface owing to screening by the metal, and the induced moments in the present Pd bilayer undergo a larger enhancement at the interface Pd layer due to the charge polarization in the dielectric material. Our results imply that Pd/MgO thin films offer the possibility for controllable spot-localized magnetic phase switching and magnetization modulation, and therefore provides a huge advantage for applications in modern magnetic data and Spintronics devices.

Acnowledgments

This work was supported by National Research Foundation of Korea (NRF) grants funded by the Korean government (MSIT) [grant numbers 2017R1A2B4012972, 2020R1A2C2013757]; and the Vietnam National Foundation for Science and Technology Development (NAFOSTED) [grant number 103.01-2019.11].

References

[1] I. Žutić, J. Fabian, and S. Das Sarma, Rev. Mod. Phys. **76**, 323 (2004).
[2] W. Eerenstein, N. D. Mathur, and J. F. Scott, Nature **442**, 759 (2006).
[3] N. A. Spaldin and M. Fiebig, Science **309**, 391 (2005).
[4] D. Chiba, M. Sawicki, Y. Nishitani, Y. Nakatani, F. Matsukura, and H. Ohno, Nature **455**, 515 (2008).
[5] M. Gajek, M. Bibes, S. Fusil, K. Bouzehouane, J. Fontcuberta, A. Barthélémy, and A. Fert, Nat. Mater. **6**, 296 (2007).
[6] E. Y. Tsymbal and H. Kohlstedt, Science **313**, 181 (2006).
[7] J. P. Velev, S. S. Jaswal, and E. Y. Tsymbal, Philos. Trans. R. Soc. A Math. Phys. Eng. Sci. **369**, 3069 (2011).
[8] J. P. Velev, C. G. Duan, J. D. Burton, A. Smogunov, M. K. Niranjan, E. Tosatti, S. S. Jaswal, and E. Y. Tsymbal, Nano Lett. **9**, 427 (2009).
[9] T. Lottermoser, T. Lonkai, U. Amann, D. Hohlwein, J. Ihringer, and M. Fiebig, Nature **430**, 541 (2004).
[10] C. G. Duan, J. P. Velev, R. F. Sabirianov, Z. Zhu, J. Chu, S. S. Jaswal, and E. Y. Tsymbal, Phys. Rev. Lett. **101**, 137201 (2008).
[11] Q. D. Odkhuu, S. H. Rhim, and S. C. Hong, Phys. Rev. B **101**, 214436 (2020).
[12] K. Nakamura, S. H. Rhim, A. Sugiyama, K. Sano, T. Akiyama, T. Ito, M. Weinert, and A. J. Freeman, Phys. Rev. B **87**, 214506 (2013).
[13] O. O. Brovko, P. Ruiz-Díaz, T. R. Dasa, and V. S. Stepanyuk, J. Phys. Condens. Matter **26**, 093001 (2014).
[14] M. K. Niranjan, C. G. Duan, S. S. Jaswal, and E. Y. Tsymbal, Appl. Phys. Lett. **96**, 222504 (2010).
[15] M. Tsujikawa, S. Haraguchi, T. Oda, Y. Miura, and M. Shirai, J. Appl. Phys. **109**, 07C107 (2011).
[16] K. H. He and J. S. Chen, J. Appl. Phys. **113**, 17C702 (2013).
[17] C. G. Duan, J. P. Velev, R. F. Sabirianov, W. N. Mei, S. S. Jaswal, and E. Y. Tsymbal, Appl. Phys. Lett. **92**, 122905 (2008).
[18] T. R. Dasa, P. A. Ignatiev, and V. S. Stepanyuk, Phys. Rev. B **85**, 205447 (2012).
[19] N. N. Negulyaev, V. S. Stepanyuk, W. Hergert, and J. Kirschner, Phys. Rev. Lett. **106**, 037202 (2011).
[20] Y. Sun, J. D. Burton, and E. Y. Tsymbal, Phys. Rev. B **81**, 064413 (2010).
[21] S. Aihara, H. Kageshima, T. Sakai, and T. Sato, J. Appl. Phys. **112**, 073910 (2012).
[22] Y. B. Kudasov and A. S. Korshunov, Phys. Lett. A **364**, 348 (2007).
[23] H. Chen, N. E. Brener, and J. Callaway, Phys. Rev. B **40**, 1443 (1989).
[24] S. C. Hong, J. Il Lee, and R. Wu, Phys. Rev. B **75**, 172402 (2007).
[25] V. L. Moruzzi and P. M. Marcus, Phys. Rev. B **39**, 471 (1989).
[26] L. Fritsche, J. Noffke, and H. Eckardt, J. Phys. F Met. Phys. **17**, 943 (2000).
[27] W. Kohn and L. J. Sham, Phys. Rev. **140**, A1133 (1965).
[28] G. Kresse and J. Furthmuller, Phys. Rev. B **54** (1996) 11169; G. Kresse and D. Joubert, Phys. Rev. B **59**, 1758 (1999).
[29] P. E. Blöchl, Phys. Rev. B **50**, 17953 (1994).
[30] T. Káňa, E. Hüger, D. Legut, M. Čák, and M. Šob, Phys. Rev. B **93**, 134422 (2016).
[31] S. S. Alexandre, M. Mattesini, J. M. Soler, and F. Yndurain, Phys. Rev. Lett. **96**, 79701 (2006).
[32] J. Goniakowski, Phys. Rev. B **59**, 11047 (1999).
[33] J. A. Rayne, Phys. Rev. **118**, 1545 (1960).
[34] J. Neugebauer and M. Scheffler, Phys. Rev. B **46**, 16067 (1992).
[35] S. Blügel, Phys. Rev. B **51**, 2025(R) (1995).
[36] A. Delin, E. Tosatti, and R. Weht, Phys. Rev. Lett. **92**, 57201 (2003).
[37] T. Taniyama, E. Ohta, and T. Sato, Europhys. Lett. **38**, 195 (1997).
[36] T. Shinohara, T. Sato, and T. Taniyama, Phys. Rev. Lett. **91**, 197201 (2003).
[38] Y. T. Jeon and G. H. Lee, J. Appl. Phys. **103**, 094313 (2008).
[39] L. Giordano, J. Goniakowski, and G. Pacchioni, Phys. Rev. B **67**, 045410 (2003).